Restriction of Signal Frequency for Thyratron Amplifier

Restriction of Signal Frequency for Thyratron Amplifier

Kazuo NOHARA,* Suemitsu MINAMOTO* and Kazuo MIYAKOSHI*

(Received November 30, 1963)

The present paper, in the first place, gives the principle to analyze the output signal of the thyratron amplifier in a double Fourier series. From this principle, the distribution of the spectra of sinusoidal frequency components, which are the compositions of the output signal of thyratron amplifier, their amplitudes and phase angles are derived. It is clarified that no harmonic component of the input signal appears in the output signal but the undesirable components, which give rise to its distortion, form spectral groups of which centers are located at even-multiples of the power source frequency. These components occur at intervals equal to the input signal frequency on either side of the center in each spectral group.

In the latter part, the maximum frequency of the input signal for the linear amplification characteristics, being attended with no distortion, is derived in a theoretical method when the thyratron amplifier is followed by the low-pass filter being endowed with the ideal sharp-cutoff characteristics. For the linear amplification characteristics of thyratron amplifier, it is to be desired, with due regard to the practical use, that the input signal has the frequency lower than a quarter of the anode power source frequency when the available filter is employed. This fact is also supported by the experimental results.

1. Introduction

Thyratron amplifiers being able to perform the power amplification by employing power switching devices such as thyratrons or silicon controlled rectifiers are very useful for automatic control and telemetry owing to its high power rating, efficiency, stability and simple circuit.

If the ratio of signal frequency to anode source one in thyratron amplifier would exceed a certain value, the distortion of the output signal is increased rapidly and lead to deviate from a linear amplification characteristics. Although considerable attention has been paid to the practical use, the theoretical analysis on the restriction of signal frequency to obtain a linear amplification has not been performed. The analysis presented in this paper for the spectra of output signal were performed by modifying the three-dimensional geometrical configuration originally developed by W. R. Bennett.[1] The distribution of the spectra of output signal is illustrated and the character (location and amplitude) of the spectra that disturb linear amplification is confirmed.

2. Principles of Analysis

As the input signal to the thyratron amplifier, a periodic voltage is assumed. In general case, the period of input signal and that of anode source are incommensurable and the output signal is nonperiodic. Such nonperiodic waveform can be analyzed by applying

* Department of Electronic Engineering, College of Engineering.

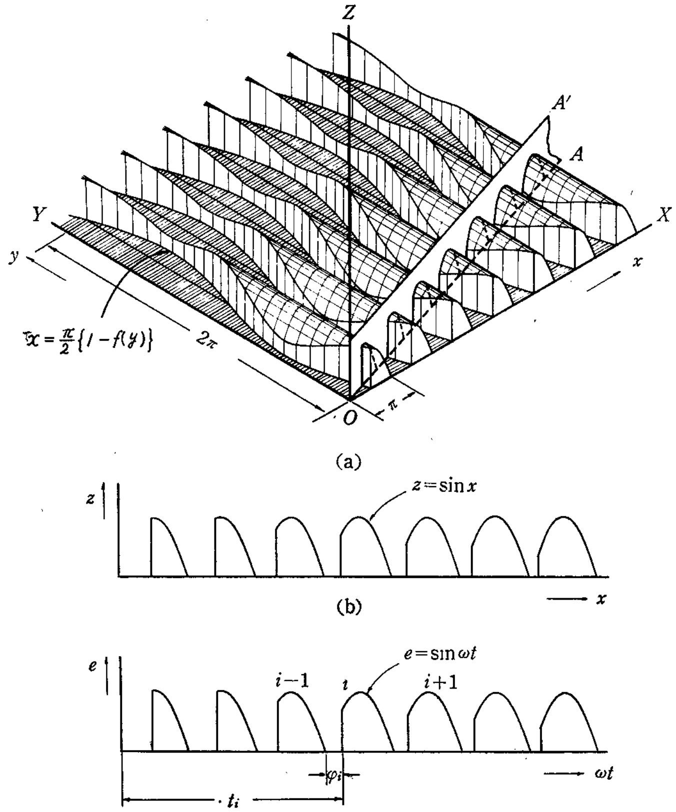

Fig. 1. Three-dimensional geometrical configuration for analyzing output signal and its resulting waveforms.

suitable modification to Bennett's three-dimensional geometrical configuration.

Though the thyratron amplifier can behave with the arbitrary waveform power source, it is practical that the sinusoidal one is applied as the anode supply voltage because of avaiable a. c. source. Then, the analysis in this paper is treated on the case the sinusoidal power source is fed to the amplifier. The diagram modified Bennett's three-dimentional geometrical configuration so that it may be in conformity with this analysis, is illustrated in the drawing of Fig. 1(a). This diagram represents part of a region in which many walls have been all parallel to each other and of identical shape. The walls rest upon a flat surface that is referred to as the XOY-plane. There is one wall for every π units of length along the X-axis. Now, consider one wall sectioned into element, the height, z, is defined by the value of $\sin x$, ended in the line represented by $x=\pi$ and its left side is the curved surface perpendicular to the XOY-plane including the curved line expressed by the relation of

$$x=\pi\{1-f(y)\}/2$$

The value of x is the difference between π and the width of the wall, measured along lines parallel to the X-axis, and $f(y)$ gives the periodic function repeated at intervals of 2π

length in the Y-direction and defined by the relation of

$$-1\leqq f(y)\leqq 1$$

Now, suppose that a AOA'-plane, perpendicular to the XOY-plane and including the origin, is passed through the walls along the line OA in the drawing. When the intersections of this plane with the walls are projected upon the XOZ-plane, likewise perpendicular to the XOY-plane but including the X-axis, the resulting shadows will have the shapes shown in Fig. 1(b) and may be thought of, on the whole, as a train of pulses. These waveforms are represented by the double periodic function of which periods are π and 2π with regard to x and y respectively. This means that the height of the configuration can be expressed as a function of x and y by means of a double Fourier series. And the double Fourier series is designated $F(x, y)$, shown as follows:

$$F(x, y)=\frac{1}{2}A_{00}+\sum_{n=1}^{\infty}(A_{on}\cos ny+B_{on}\sin ny)+\sum_{m=1}^{\infty}(A_{mo}\cos 2mx+B_{mo}\sin 2mx)$$
$$+\sum_{m=1}^{\infty}\sum_{n=\pm 1}^{\pm\infty}\{A_{mn}\cos(2mx+ny)+B_{mn}\sin(2mx+ny)\} \quad (1)$$

where,

$$A_{mn}+jB_{mn}=\frac{1}{\pi^2}\int_0^{2\pi}\int_0^{\pi}F(x, y)\varepsilon^{j(2mx+ny)}\cdot dxdy \quad (2)$$
$$(m=0,\ 1,\ 2,\ 3,\ \cdots\cdots,\ n=0,\ 1,\ 2,\ 3,\ \cdots\cdots)$$

In Eq. (1), $F(x,y)$ has the value of zero for x within the restriction of $0\leqq x<\pi\{1-f(y)\}/2$, and $\sin x$ for x of $\pi\{1-f(y)\}/2\leqq x\leqq\pi$. And therefore, Eq. (2) may be written as the following equation.

$$A_{mn}+jB_{mn}=\frac{1}{\pi^2}\int_0^{2\pi}\int_{\pi\{1-f(y)\}/2}^{\pi}\sin x\cdot\varepsilon^{j(2mx+ny)}\,dxdy \quad (3)$$
$$(m=0,\ 1,\ 2,\ 3,\ \cdots\cdots,\ n=0,\ 1,\ 2,\ 3,\ \cdots\cdots)$$

If x and y may be regarded as phase angles instead of distance as expressed in Eq. (4)

$$\left.\begin{aligned}x&=\omega t\\ y&=\alpha t\end{aligned}\right\} \quad (4)$$

and the slope of OA is ratio between α to ω, the projected shapes shown in Fig. 1(b) may be thought of as a train of rectified sine wave in which only the leading edge is varied as to $\pi f(\alpha t)/2$, as shown in Fig. 1(c). Referring to Fig. 1(a) and (c), next relation is satisfied at the instance of t_i when the leading edge of arbitrary i-th pulsation occurs.

$$\varphi_i=\pi\{1-f(\alpha t_i)\}/2 \quad (5)$$

where, φ_i stands for the phase angle of ignition of the i-th pulsation, and $0\leqq\varphi_i\leqq\pi$. The expression for φ_i given by Eq. (5) is identical to that of the ignition phase angle of the output signal in thyratron amplifier controlled by the saw-tooth bias voltage and input signal given by $A'f(\alpha t)$.[2] The basic circuit of thyratron amplifier with saw-tooth bias voltage is shown in Fig. 2. Thyratrons, Th_1 and Th_2, connected in a single-phase full wave rectifier type with respect to the anode source voltage, $E_m \sin \omega t$, are controlled by the resultant voltage of input signal, $A'f(\alpha t)$, and the saw-tooth bias voltage, of which period is equal to a half of that of anode source voltage and peak to peak value is $2A'$. The output voltage, $E(t)$, of this amplifier can be expressed as Eq. (6) by inserting the relationship of Eq. (4) into Eq. (1).

$$E(t)=\frac{1}{2}A_{00}+\sum_{n=1}^{\infty}\{A_{on}\cos(n\alpha t)+B_{on}\sin(n\alpha t)\}+\sum_{m=1}^{\infty}\{A_{mo}\cos(2m\omega t)+B_{mo}\sin(2m\omega t)\}$$
$$+\sum_{m=1}^{\infty}\sum_{n=\pm 1}^{\pm\infty}\{A_{mn}\cos(2m\omega+n\alpha)t+B_{mn}\sin(2m\omega+n\alpha)t\}. \tag{6}$$

In Eq. (6), the first term $A_{00}/2$ is d.c. component of the output voltage. The frequency components of the second term correspond to the fundamental one of input signal voltage and its harmonics. The third term gives the even-multiple components of anode source frequency. And the fourth term represents the harmonic components located, in the spectra of output signal, on either side of the spectrum given by the third term at intervals of α. In other words, frequencies of the components represented with this term are the sum and difference of even-multiples of anode source frequency and integral-multiples of input signal one. Assuming that the maximum value of the anode voltage is unity, the amplitude of each component may be given from Eq. (3).

Now, consider the output waveform of another thyratron amplifier, of which average load voltage is proportional to the input signal voltage and instantaneous load voltage is to be analyzed in the following sections, having an input signal voltage $E_c \sin \alpha t$ as shown in Fig. 3. This thyratron amplifier has the same circuit as that of Fig. 2 except that the saw-tooth bias voltage in the control grid circuit is replaced with the sinusoidal one given by Eq. (7).

$$g(\omega t)=\frac{E_m}{k}\left[\int_0^{\omega t}\sin\omega t\,d\omega t-\frac{1}{2}\int_0^{\pi}\sin\omega t\,d\omega t\right]=-\frac{E_m}{k}\cos\omega t=-A\cos\omega t \tag{7}$$

where, k is an arbitrary constant indicating the ratio of E_m/A.

In order that thyratron amplifier can play a role normally without saturation, the amplitude of input signal E_c must be not larger than that of the specified bias voltage A at any occasion. Assuming that M stands for the ratio of E_c to A and $0 \leqq M \leqq 1$, next

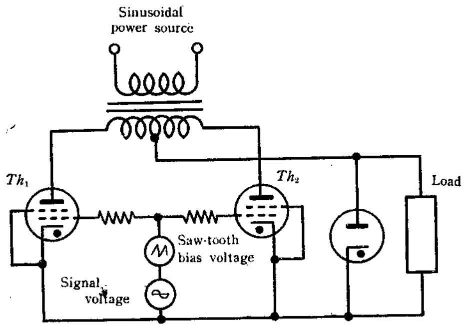

Fig. 2. Basic circuit of thyraton amplifier with saw-tooth bias voltage.

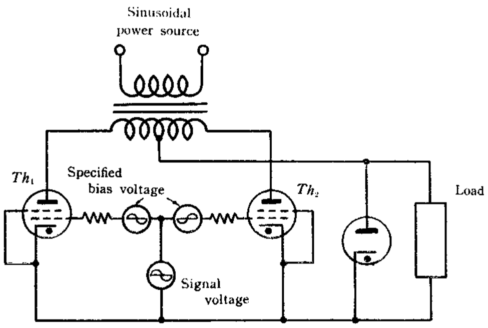

Fig. 3. Basic circuit of thyratron amplifier with specified bias voltage.

equation is to be satisfied at the instance t_p that the ignition occurs in an arbitrary p-th positive half cycle of the anode supply voltage.

$$\cos\varphi_p = M\sin\alpha t_p \tag{8}$$

where, φ_p is the firing angle in the p-th positive half cycle and $0\leqq\varphi_p\leqq\pi$.

On the other hand, if the input signal, $A'f(\alpha t)$, of saw-tooth method thyrtron amplifier shown in Fig. 2 is that of Eq. (9),

$$A'f(\alpha t) = A'[1-\{2\,\mathrm{Cos}^{-1}(M\sin\alpha t)/\pi\}] \tag{9}$$

at the instance of ignition in the p-th positive half cycle, the relation of Eq. (10) is derived from Eq. (5) and Eq. (9)

$$\cos\varphi'_p = M\sin\alpha t'_p \tag{10}$$

where, φ'_p is the firing angle in the p-th positive half cycle and $0\leqq\varphi'_p\leqq\pi$.

Referring to Eq. (8) and Eq. (10), it is apparent that the output signal waveform obtained by applying a simple sinusoidal input signal, $AM\sin\alpha t$, to the thyratron amplifier shown in Fig. 3 is identical with that of saw-tooth method thyratron amplifier shown in Fig. 2 with provisos that the input signal represented by Eq. (9) and the identical anode voltage with the former must be employed. In this case, the spectra of output signal obtained from each thyratron amplifier ought to be identical, of which distribution and amplitudes can be derived from Eq. (6) and Eq. (3), respectively, by inserting Eq. (11).

$$f(y) = 1-\{2\,\mathrm{Cos}^{-1}(M\sin y)/\pi\} \tag{11}$$

3. Calculation of Harmonic Component Amplitudes in Output Signal

Referring to Eq. (3), Eq. (4) and Eq. (11), the amplitudes of all components in the output signal yielded when the simple sinusoidal input signal, $AM\sin\alpha t$, is fed into thyratron amplifier of Fig. 3, they are corresponding to all termes expressed in Eq. (6), can be calculated, provided that the maximum value of anode voltage is unity, as follows:

i. D. C. component

The d. c. component, $A_{00}/2$, in the output signal is given by Eq. (12) with a simple procedure of inserting $m=0$, $n=0$ into Eq. (3)

$$\frac{A_{00}}{2} = \frac{1}{2\pi^2}\int_0^{2\pi}\int_{\mathrm{Cos}^{-1}(M\sin y)}^{\pi}\sin x\,dx\,dy = \frac{1}{2\pi^2}\int_0^{2\pi}(1+M\sin y)\,dy = \frac{1}{\pi} \tag{12}$$

ii. Component corresponding to Signal Frequency

The component corresponding to the signal frequency is given by Eq. (13) when $m=0$ and $n=1$ in Eq. (3).

$$A_{01}+jB_{01} = \frac{1}{\pi^2}\int_0^{2\pi}\int_{\mathrm{Cos}^{-1}(M\sin y)}^{\pi}\sin x\cdot\varepsilon^{jy}\,dx\,dy = \frac{1}{\pi^2}\int_0^{2\pi}(1+M\sin y)\varepsilon^{jy}\,dy = j\frac{M}{\pi} \tag{13}$$

iii. Harmonic Components of Signal Frequency

By inserting $m=0$, $n\geqq2$ into Eq. (3), the harmonic components are given by following equation.

$$A_{on}+jB_{on}=\frac{1}{\pi^2}\int_0^{2\pi}\int_{\mathrm{Cos}^{-1}(M\sin y)}^{\pi}\sin x\cdot\varepsilon^{jny}dxdy=\frac{1}{\pi^2}\int_0^{2\pi}(1+M\sin y)\cdot\varepsilon^{jny}dy=0 \tag{14}$$

From Eq. (14), it is apparent that harmonic components do not appear in the output signal of thyratrom amplifier.

iv. Even-Multiple Harmonics of Anode Source Frequency

By insreting $m\geqq1$ and $n=0$ into Eq. (3), amplitudes of the even-multiple harmonics of anode source frequency, which are indicated by the third term in Eq. (6) are represented as follows:

$$\begin{aligned}A_{mo}+jB_{mo}&=\frac{1}{\pi^2}\int_0^{2\pi}\int_{\mathrm{Cos}^{-1}(M\sin y)}^{\pi}\sin x\cdot\varepsilon^{j2mx}dxdy\\
&=\frac{-2}{\pi^2(4m^2-1)}\int_0^{2\pi}\Big[\frac{1}{2}-\exp\{j2m\,\mathrm{Cos}^{-1}(M\sin y)\}\,[jm\sin\{\mathrm{Cos}^{-1}(M\sin y)\}\\
&\qquad-\frac{1}{2}\cos\{\mathrm{Cos}^{-1}(M\sin y)\}]\Big]dy\\
&=\frac{-1}{\pi^2(4m^2-1)}\int_0^{2\pi}dy\\
&\qquad+\frac{1}{2\pi^2(4m^2-1)}\int_0^{2\pi}[(2m-1)\cos\{(2m+1)\,\mathrm{Cos}^{-1}(M\sin y)\}\\
&\qquad-(2m+1)\cos\{(2m-1)\,\mathrm{Cos}^{-1}(M\sin y)\}]dy\\
&\qquad+\frac{1}{2\pi^2(4m^2-1)}\int_0^{2\pi}[(2m-1)\sin\{(2m+1)\,\mathrm{Cos}^{-1}(M\sin y)\}\\
&\qquad-(2m+1)\sin\{(2m-1)\,\mathrm{Cos}^{-1}(M\sin y)\}]dy\end{aligned} \tag{15}$$

where, the terms of $\cos\{(2m+1)\,\mathrm{Cos}^{-1}(M\sin y)\}$ and $\cos\{(2m-1)\,\mathrm{Cos}^{-1}(M\sin y)\}$ expanded respectively as follows:

$$\left.\begin{aligned}&\cos\{(2m+1)\,\mathrm{Cos}^{-1}(M\sin y)\}\\
&=\frac{1}{2}(2M\sin y)^{2m+1}+\frac{1}{2}\sum_{r=1}^{m}(-1)^r\frac{2m+1}{r!}\Big[\prod_{k=r+1}^{2r-1}(2m-k+1)\Big](2M\sin y)^{2(m-r)+1}\\
&\cos\{(2m-1)\,\mathrm{Cos}^{-1}(M\sin y)\}\\
&=\frac{1}{2}(2M\sin y)^{2m-1}+\frac{1}{2}\sum_{r=1}^{m-1}(-1)^r\frac{2m-1}{r!}\Big[\prod_{k=r+1}^{2r-1}(2m-k-1)\Big](2M\sin y)^{2(m-r)-1}\end{aligned}\right\} \tag{16}$$

and the value of second term in Eq. (15) results in zero because the relation of Eq. (17) is approved.

$$\int_0^{2\pi}\sin^{2s+1}y\,dy=0 \tag{17}$$

Therefore, the real term, A_{mo}, of Eq. (15) is given by Eq. (18).

$$A_{mo}=\frac{-1}{\pi^2(4m^2-1)}\int_0^{2\pi}dy=\frac{-2}{\pi(4m^2-1)} \tag{18}$$

The imaginary term, B_{mo}, is given by Eq. (19) by expanding $\sin\{(2m+1)\,\mathrm{Cos}^{-1}(M\sin y)\}$ and $\sin\{(2m-1)\,\mathrm{Cos}^{-1}(M\sin y)\}$ into the infinite power series with respect to $M\sin y$,

$$B_{mo}=\frac{(-1)^m}{2\pi^2(4m^2-1)}\int_0^{2\pi}\Big[(2m-1)\Big\{1-(2m+1)^2$$

$$\times\sum_{r=1}^{\infty}\frac{(2^2-\overline{2m+1}^2)(4^2-\overline{2m+1}^2)\cdots(\overline{2r-2}^2-\overline{2m+1}^2)}{(2r)!}(M\sin y)^{2r}\Big\}$$

$$+(2m+1)\Big\{1-(2m-1)^2\sum_{r=1}^{\infty}\frac{(2^2-\overline{2m-1}^2)(4^2-\overline{2m-1}^2)\cdots(\overline{2r-2}^2-\overline{2m-1}^2)}{(2r)!}$$

$$\times(M\sin y)^{2r}\Big]dy$$

$$=\frac{(-1)^m4m}{2\pi^2}\int_0^{2\pi}\Big[\frac{1}{4m^2-1}-\sum_{r=1}^{\infty}\frac{(1^2-4m^2)(3^2-4m^2)\cdots(\overline{2r-3}^2-4m^2)}{(2r)!}(M\sin y)^{2r}\Big]dy$$

$$=\frac{(-1)^m4m}{\pi}\Big[\frac{1}{4m^2-1}-\sum_{r=1}^{\infty}\frac{(1^2-4m^2)(3^2-4m^2)\cdots(\overline{2r-3}^2-4m^2)}{(r!)^2}\Big(\frac{M}{2}\Big)^{2r}\Big] \tag{19}$$

The amplitudes of harmonic components, of which frequencies are equal to the even-multiple of anode source frequency, are given by the next equation.

$$A_{mo}+jB_{mo}=\frac{1}{\pi}\Big[\frac{-2}{4m^2-1}+(-1)^m j4m\Big\{\frac{1}{4m^2-1}$$

$$-\sum_{r=1}^{\infty}\frac{(1^2-4m^2)(3^2-4m^2)\cdots(\overline{2r-3}^2-4m^2)}{(r!)^2}\Big(\frac{M}{2}\Big)^{2r}\Big\}\Big] \tag{20}$$

v. Components corresponding to Sum and Difference of Even-Multiples of Anode Source Freqnency and Integral Multiples of Input Signal Frequency

By inserting $m\geqq 1$, $n\geqq 1$ into Eq. (3), the amplitudes of components, $A_{mn}+jB_{mn}$, indicated by the fourth term in Eq. (6) and located, in the spectra of output signal, at distances of integral multiples of input signal frequency from the position of even-multiples of anode source frequency are represented by Eq. (21).

$$A_{mn}+jB_{mn}=\frac{1}{\pi^2}\int_0^{2\pi}\int_{\mathrm{Cos}^{-1}(M\sin y)}^{\pi}\sin x\cdot\varepsilon^{j(2mx+ny)}dxdy$$

$$=\frac{-2}{\pi^2(4m^2-1)}\int_0^{2\pi}\varepsilon^{jny}\Big[\frac{1}{2}-\exp\{j2m\,\mathrm{Cos}^{-1}(M\sin y)\}\,[jm\sin\{\mathrm{Cos}^{-1}(M\sin y)\}$$

$$-\frac{1}{2}\cos\{\mathrm{Cos}^{-1}(M\sin y)\}]\Big]dy$$

$$=\frac{1}{2\pi^2(4m^2-1)}\Big[\int_0^{2\pi}\cos ny[(2m-1)\cos\{(2m+1)\,\mathrm{Cos}^{-1}(M\sin y)\}$$

$$-(2m+1)\cos\{(2m-1)\,\mathrm{Cos}^{-1}(M\sin y)\}]dy$$

$$-\int_0^{2\pi}\sin ny[(2m-1)\sin\{(2m+1)\,\mathrm{Cos}^{-1}(M\sin y)\}$$

$$-(2m+1)\sin\{(2m-1)\,\mathrm{Cos}^{-1}(M\sin y)\}]dy$$

$$+j\int_0^{2\pi}\sin ny[(2m-1)\cos\{(2m+1)\,\mathrm{Cos}^{-1}(M\sin y)\}$$

$$-(2m+1)\cos\{(2m-1)\,\mathrm{Cos}^{-1}(M\sin y)\}]dy$$

$$+j\int_0^{2\pi}\cos ny[(2m-1)\sin\{(2m+1)\,\mathrm{Cos}^{-1}(M\sin y)\}$$

$$-(2m+1)\sin\{(2m-1)\,\mathrm{Cos}^{-1}(M\sin y)\}]dy\Big] \tag{21}$$

The first term in the bracket of Eq. (21) can be calculated by expanding $\cos\{(2m+1)\times\mathrm{Cos}^{-1}(M\sin y)\}$ and $\cos\{(2m-1)\,\mathrm{Cos}^{-1}(M\sin y)\}$ into power series with respect to $2M\sin y$ and is equal to zero. And by expanding $\sin\{(2m+1)\,\mathrm{Cos}^{-1}(M\sin y)\}$ and $\sin\{(2m-1)\times\mathrm{Cos}^{-1}(M\sin y)\}$ into infinite series, the second term is given by Eq. (22).

$$(-1)^m 4m(4m^2-1)\int_0^{2\pi}\sin ny\Big\{\frac{1}{4m^2-1}-\sum_{r=1}^{\infty}\frac{(1^2-4m^2)(3^2-4m^2)\cdots(\overline{2r-3}^2-4m^2)}{(2r)!}(M\sin y)^{2r}\Big\}dy \tag{22}$$

As the relation of Eq. (23) is approved, the integration of the second term in Eq. (21) becomes zero.

$$\int_0^{2\pi}\sin ny\sin^{2r}y\,dy=0 \tag{23}$$

Then, the value of the real term, A_{mn}, in Eq. (21) ought to be zero. The value of imaginary term, B_{mn}, can be calculated from the third term and the fourth in like manner mentioned above and given by Eq. (24)

$$\begin{aligned}&\frac{1}{2}\int_0^{2\pi}\sin ny\Big[(2m-1)(2M\sin y)^{2m+1}+(4m^2-1)\sum_{r=1}^{m}\frac{(-1)^r}{r!}\Big[\prod_{k=r+1}^{2r-1}(2m-k+1)\Big]\\&\times(2M\sin y)^{2(m-r)+1}-(2m+1)(2M\sin y)^{2m-1}-(4m^2-1)\\&\times\sum_{r=1}^{m-1}\frac{(-1)^r}{r!}\Big[\prod_{k=r+1}^{2r-1}(2m-k-1)\Big](2M\sin y)^{2(m-r)-1}\Big]dy\\&=m(4m^2-1)\sum_{r=0}^{m}\Big[(-1)^r\frac{(2m-r-1)!}{r!(2m-2r+1)!}(2M)^{2(m-r)+1}\int_0^{2\pi}\sin ny\sin^{2(m-r)+1}y\,dy\Big]\end{aligned} \tag{24}$$

In general, $\sin^{2s+1}y$ is expanded in the form of the following equation.

$$\sin^{2s+1}y=\frac{1}{2^{2s}}\sum_{l=0}^{s}(-1)^{s+l}\binom{2s+1}{l}\sin(2s-2l+1)y$$

When n is even or n is odd number larger than $2(m-r)+1$, in other words r is larger than $m-(n-1)/2$, the following relation is approved.

$$\int_0^{2\pi}\sin ny\cdot\sin^{2(m-r)+1}y\,dy=0$$

When n is odd and $n\leqq 2(m-r)+1$, or $r\leqq m-(n-1)/2$,

$$\int_0^{2\pi}\sin ny\cdot\sin^{2(m-r)+1}y\,dy=\frac{(-1)^{(n-1)/2}}{2^{2(m-r)}}\binom{2(m-r)+1}{m-r-(n-1)/2}\pi$$

is approved. The third term in the bracket of Eq. (21) is zero if n is even. If n is odd, it may be expressed as follows:

$$2\pi m(4m^2-1)(-1)^{(n-1)/2}\sum_{r=0}^{m-(n-1)/2}\Big[(-1)^r M^{2(m-r)+1}\times\frac{(2m-r-1)!}{r!\{m-r-(n-1)/2\}!\,\{m-r+(n+1)/2\}!}\Big] \tag{25}$$

This may be briefly summarized in the following outline. The value of the third term in

Eq. (21) is zero in both cases that n is even and n is odd, $n>2m+1$. If n is odd, $n\leqq 2m+1$, it may be expressed as Eq. (25), The fourth term of Eq. (21) is given by the following expression by adopting the similar step to Eq. (19).

$$(-1)^{m+1}4m(4m^2-1)\sum_{r=1}^{\infty}\left[\frac{(1^2-4m^2)(3^2-4m^2)\cdots(\overline{2r-3}^2-4m^2)}{(2r)!}M^{2r}\int_0^{2\pi}\cos ny\sin^{2r}ydy\right] \tag{26}$$

where,

$$\sin^{2r}y=\frac{1}{2^{2r-1}}\left[\sum_{l=0}^{r-1}(-1)^{r+l}\binom{2r}{l}\cos(2r-2l)y+\frac{1}{2}\binom{2r}{r}\right]$$

If n is odd or n is even, $r<n/2$;

$$\int_0^{2\pi}\cos ny\cdot\sin^{2r}ydy=0$$

If n is even, $r\geqq n/2$;

$$\int_0^{2\pi}\cos ny\cdot\sin^{2r}ydy=\frac{(-1)^{n/2}}{2^{2r-1}}\binom{2r}{r-(n/2)}\pi$$

is approved. Therefore, the integration of the fourth term in the bracket of Eq. (21) is zero when n is odd, and if n is even it is expressed as follows:

$$(-1)^{m+(n/2)+1}\cdot 8\pi m(4m^2-1)\sum_{r=n/2}^{\infty}\left[\frac{(1^2-4m^2)(3^2-4m^2)\cdots(\overline{2r-3}^2-4m^2)}{(2r)!}\left(\frac{M}{2}\right)^{2r}\binom{2r}{r-(n/2)}\right]$$

$$=(-1)^{m+(n/2)+1}\cdot 8\pi m(4m^2-1)\sum_{r=n/2}^{\infty}\frac{(1^2-4m^2)(3^2-4m^2)\cdots(\overline{2r-3}^2-4m^2)}{\{r+(n/2)\}!\,\{r-(n/2)\}!}\left(\frac{M}{2}\right)^{2r} \tag{27}$$

Referring to Eq. (21)～Eq. (27), $A_{mn}+jB_{mn}$ may be expressed as follows:

when n is odd and $n\leqq 2m+1$,

$$A_{mn}+jB_{mn}$$
$$=j(-1)^{(n-1)/2}\frac{m}{\pi}\sum_{r=0}^{m-(n-1)/2}\left[(-1)^r M^{2(m-r)+1}\frac{(2m-r-1)!}{r!\{m-r-(n-1)/2\}!\,\{m-r+(n+1)/2\}!}\right] \tag{28}$$

when n is odd and $n>2m+1$,

$$A_{mn}+jB_{mn}=0 \tag{29}$$

when n is even,

$$A_{mn}+jB_{mn}$$
$$=j(-1)^{m+(n/2)+1}\frac{4m}{\pi}\sum_{r=n/2}^{\infty}\left[\frac{(1^2-4m^2)(3^2-4m^2)\cdots(\overline{2r-3}^2-4m^2)}{\{r+(n/2\}!\,\{r-(n/2)\}!}\left(\frac{M}{2}\right)^{2r}\right] \tag{30}$$

4. Restriction of Signal Frequency

In the above mentioned calculation, it was founded that there was no harmonic component of signal frequency but undesired frequency components distributed on either side of even multiples of anode source frequency in the output spectra. These undesired frequency components located at intervals of signal frequency in the spectra give rise to distortions which cause the deviation from the linear output characteristics of thyratron amplifier.

Fig. 4 shows the amplitudes of frequency components calculated with digital computer for the range from zero to five of m and various value of M, assuming the ratio of ω to α is 10. The variation in value of ω/α shifts only the relative positions of frequency component corresponding to signal frequency and those distributed in the vicinity of even-multiples of anode source frequency of which amplitudes are kept constant.

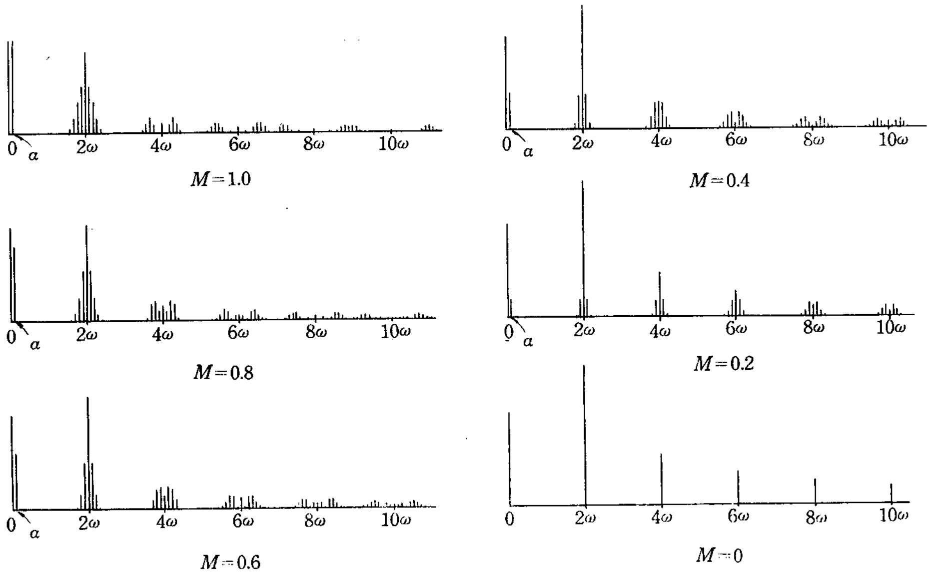

Fig. 4. Spectra of the output signal of thyraton amplifier.

It is interpreted that the amplitudes of undesired frequency components mentioned above, in general, are decreased rapidly as the center frequency (even-mutiple frequency of anode voltage) increases. The frequency components having relatively high frequency among these undesired components, of which amplitude is much smaller than that corresponding to signal frequency and locations are in far distance from it, may be eliminated from the output signal by employing a well-designed low-pass filter between thyratron amplifier and the load so that they may not affect the linear amplification characteristics. It is noted that the undesired frequency components having the possibility of exerting the bad influence upon the linear characteristics of thyratron amplifier are those which occur in the vicinity of the second harmonic component of anode source frequency. And the character of these components will be studied in the following expressions.

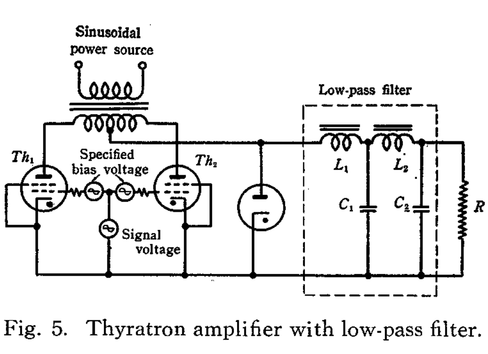

Fig. 5. Thyratron amplifier with low-pass filter.

The value of $B_{1,0}$ in the second harmonic component of anode source frequency which may be calculated with inserting $m=1$ into the third term of Eq. (15) and evaluating its integral, is given by the following expression rather than the infinite series form obtained from Eq. (20).

$$B_{1,0}=\frac{1}{6\pi^2}\int_0^{2\pi}[\sin\{3\,\mathrm{Cos}^{-1}(M\sin y)\}-3\sin\{\mathrm{Cos}^{-1}(M\sin y)\}]dy$$
$$=\frac{-8}{3\pi^2}\int_0^{\pi/2}(1-M^2\sin^2 y)dy=\frac{-8}{(3\pi)^2}\{2(2-M^2)E(M)-(1-M^2)K(M)\} \qquad (31)$$

where, $K(M)$ and $E(M)$ indicate the complete elliptic integral of the first kind and the second, respectively Referring to Eq. (18) and Eq. (31), the absolute value of the second harmonic component of anode source frequency is given by

$$\sqrt{A_{1,0}^2+B_{1,0}^2}=\frac{2}{3\pi}\sqrt{1+\left(\frac{2}{3\pi}\right)^2\{4(2-M^2)E(M)-2(1-M^2)K(M)\}^2} \qquad (32)$$

The frequency components located at intervals of the signal frequency, with the second harmonic component of anode source frequency as their center, can be separated into two groups in which n is odd and even as mentioned in the previous section. From Eq. (29), if n is odd number, only the components of $B_{1,1}$ and $B_{1,3}$ are in existence, of which amplitudes are represented as follows:

$$B_{1,1}=(M^3-2M)/2\pi \qquad (33)$$

$$B_{1,3}=M^3/6\pi \qquad (34)$$

If n is even numbers, $B_{1,n}$-components are in existence for the even numbers of $2\leqq n\leqq\infty$, according to the theoretical analysis as shown in Eq. (30). The frequency components of $B_{1,n}$ may be considered to occur over the infinite frequency band-width. Referring to Eq. (30), the values of $B_{1,n}$ are on simple decrease regardless of the value of n being even. Each maximum value of $B_{1,n}$ is expressed with Eq. (35), by inserting $M=1$ into the fourth term in bracket of Eq. (21) and evaluating the integral.

$$B_{1,n(\max.)}=16/(n^2-3^2)(n^2-1^2)\pi^2 \qquad (35)$$

Eq. (35) shows that the maximum value of $B_{1,n}$ decreases rapidly according to the increase of n.

By making use of Eq. (30) ~ Eq. (35), the ratio between the amplitude of each frequency component to that corresponding to signal frequency is given as a function of M in Fig. 6. It may be found in Fig. 6 that the amplitude of $B_{1,n}$ decreases rapidly according to increase of n and decrease of M. For example, its value for $n=6$, $M=1$ is observed as 0.54 per cent of the component corresponding to signal frequency. When n is larger than six, its value is so small that it may be neglected in practical use. From practical point of view, the frequency band-width of the undesired frequency components located in the vicinity of the second harmonic component of anode source frequency may be considered to be the region of $2\omega\pm6\alpha$. And it may be considered that no undesired frequency component to distort the output signal is in the frequency region lower than $2\omega-6\alpha$.

On the basis of the theoretical analysis mentioned above, the distributions of undesired frequency components for $M=1$, in the neighbour of the signal frequency are shown in Fig. 7(a) and (b). Fig. 7(a) shows the distribution for the case that the signal frequency is sufficiently small compared with the anode voltage one. The undesired frequency components giving bad influence to the amplification characteristics form a cluster in the vicinity of the second harmonic component of anode source frequency, may be eliminated by a proper filter. If the signal frequency is relatively high as shown in Fig. 7(b), the undesirable frequency components may be distributed in wider region so far from the second harmonic component of anode source frequency that some of them may come close to the signal frequency or get into the lower frequency region than it. In such a case, it becomes difficult to eliminate all of

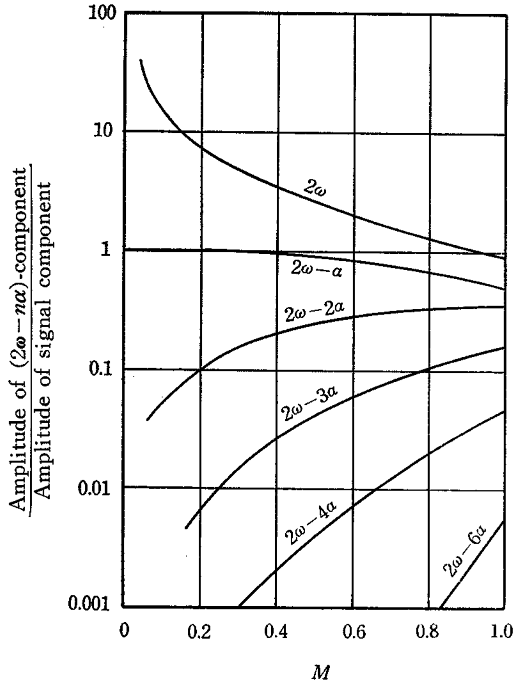

Fig. 6. Ratio of $(2\omega-n\alpha)$-components to signal component in output signal for various values of M.

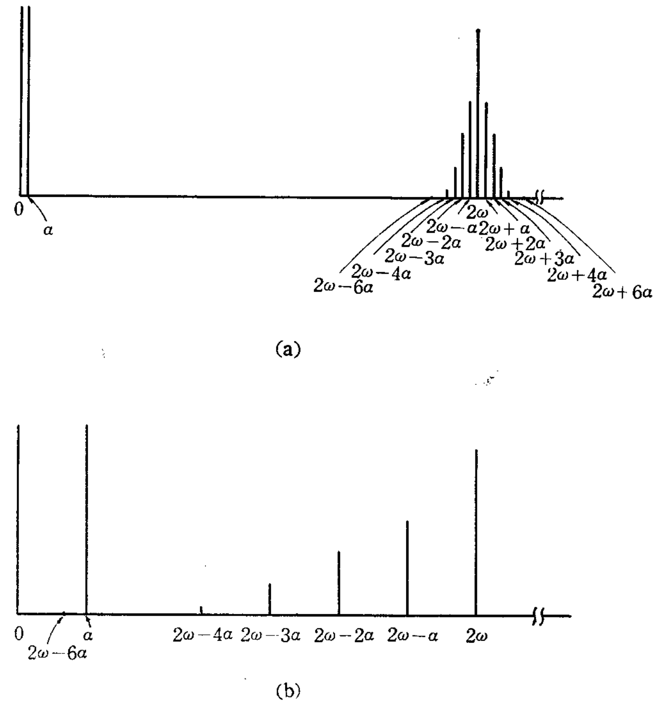

Fig. 7. Spectra in the vicinity of second-harmonic component of anode source frequency.

the undesired frequency componts even if the filter may be employed and those left from filtering give rise to the distortion component in the output signal. Thyratron amplifier can perform the ideal linear amplification without distortion for the ultra low frequency signals of which frequencies are sufficiently low but brings the distortion on its output signal, which loses the linear amplification characteristics, for the signals having higher frequencies than a certain value.

The upper limit of input signal frequency that can be amplified without distortion is swayed also by the characteristics of filter employed and can not be determined readily, However, it may be considered that the undesired components do not occur in the lower frequency region than the frequency of $2\omega-6\alpha$ in practical use as mentioned above, and therefore the linear amplifications of the ultra low frequency signals, having the frequency lower than $2\omega/7$, can be performed without distortion by thyratron amplifier with the low-pass filter having ideal sharp cutoff characteristics.

Practically, if the low-pass filter having cutoff frequency of $2\omega/8$ and attenuation of $24db/oct.$ is employed, all undesired frequency components besides the even-multiple frequency components of anode voltage are less than 0.04 per cent of the component corresponding to signal frequency. The value of the second harmonic component of the anode source frequency, which is the largest one of all even-multiple frequency components of it and increased according to decreasing of M, is about 0.021 per cent of the component corresponding to signal frequency for $M=1$ and does not exceed 0.36 per cent for $M=0.1$. Since thyratron amplifier is designed, in general, so that it may not work under the condition that M is extremely small, the frequency component of 2ω is sufficiently small compared with that of α and can be neglected in practical use. It is noted that the ultra low frequency signals having the frequencies lower than $2\omega/8$ can be amplified without distortion if thyratron amplifier is followed by a proper low-pass filter.

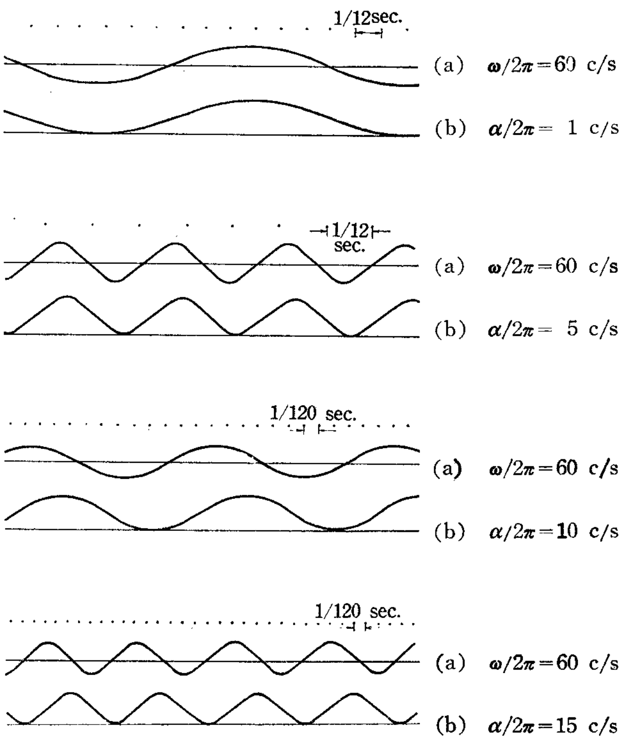

(a) input signal (b) output signal

Fig. 8. Oscillograms of output signals.

Fig. 8 shows the oscillograms of output voltage for input signals having various frequencies, which is observed with thyratron amplifier employing two L-type low-pass filters connected in cascade as shown iu Fig. 5. The values of elements composing these filters must be determined so that thyratron amplifier may behave in normal manner,[3] in other words, the current flowing through two inductors of the filter may be continuous. The attenuation characteristics of low-pass filter measured for the load resistance which is used in this experiment are shown in Fig. 9. It will be seen from the oscillograms in Fig. 8 that thyratron amplifier has the ideal linear amplification characteristics for input signals of which frequencies are lower than $2\omega/8$.

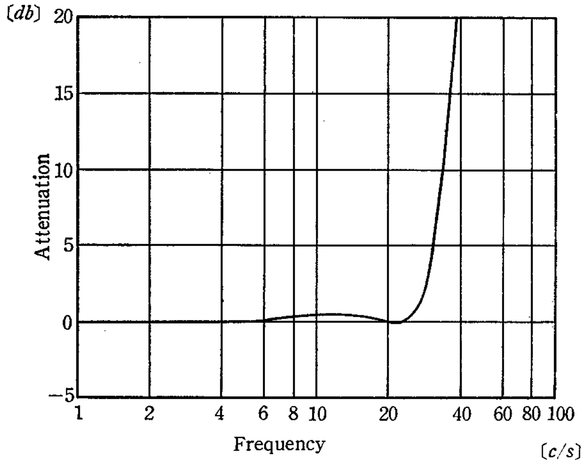

Fig. 9. Attenuation characteristics of low-pass filter used in experimental amplifier of Fig. 5.

5. Conclusions

It has been known that there are certain restrictions on the maximum frequency of ultra low frequency input signal which may be amplified without distortion by thyratron amplifier. However, it has not been analyzed in theoretical method.

In order to give the basis of determining the maximum frequency of input signal, the spectra of output signal in thyratron amplifier were analyzed by modifying the three-dimensional geometrical configuration developed by W. R. Bennett. From the analysis in this report, the character of the frequency components causing the distortion in the output signal was revealed. The maximum frequency of input signal to be amplified without distortion by thyratron amplifier was determined by theoretical method. And these results were confirmed by experiments. The analysis gave the results mentioned above as well as the useful data to design the filter to be connected to thyratron amplifier by clarifying the distribution of spectra in the output signal. It is sure to be useful ground for the development in the practical use of thyratron amplifier.

Appendix

Derivation of Eq. (1) and Eq. (2).

Now, suppose that a plane instead of AOA'-plane, perpendicular to the XOY-surface and including the straight line $y=y_1$, parallel to the X-axis, is passed through the walls. When the intersections of this plane with the walls are projected upon XOZ-plane, the resulting shadows will be, as a whole, a train of pulses, each of them having the identical shape. This train of pulses is periodic with respect to x in intervals of π and the resulting figure, $F(x, y_1)$, may be represented by a simple Fourier series as follows:

$$F(x, y_1)=\frac{1}{2}a_0(y_1)+\sum_{m=1}^{\infty}\{a_m(y_1)\cos 2mx+b_m(y_1)\sin 2mx\} \tag{36}$$

where,

$$a_m(y_1)=\frac{2}{\pi}\int_0^{\pi}F(x, y_1)\cos 2mxdx \tag{37}$$

$$b_m(y_1)=\frac{2}{\pi}\int_0^{\pi}F(x, y_1)\sin 2mxdx \tag{38}$$

$$(m=0,\ 1,\ 2,\ 3,\ \cdots\cdots)$$

The values of the coefficients $a_m(y_1)$ and $b_m(y_1)$ depend upon that of y_1 and are periodic with respect to y in intervals of 2π. In general, $a_m(y)$ and $b_m(y)$ may be expanded into the simple Fourier series as follows:

$$a_m(y)=\frac{1}{2}c_{mo}+\sum_{n=1}^{\infty}(c_{mn}\cos ny+d_{mn}\sin ny) \tag{39}$$

$$b_m(y)=\frac{1}{2}c'_{mo}+\sum_{n=1}^{\infty}(c'_{mn}\cos ny+d'_{mn}\sin ny) \tag{40}$$

$$(m=0,\ 1,\ 2,\ 3,\ \cdots\cdots)$$

where,

$$c_{mn}=\frac{1}{\pi}\int_0^{2\pi}a_m(y)\cos nydy \tag{41}$$

$$d_{mn}=\frac{1}{\pi}\int_0^{2\pi}a_m(y)\sin nydy \tag{42}$$

$$c'_{mn}=\frac{1}{\pi}\int_0^{2\pi}b_m(y)\cos nydy \tag{43}$$

$$d'_{mn}=\frac{1}{\pi}\int_0^{2\pi}b_m(y)\sin nydy \tag{44}$$

$$(m=0,\ 1,\ 2,\ 3,\ \cdots\cdots,\quad n=0,\ 1,\ 2,\ 3,\ \cdots\cdots)$$

From Eq. (37) and Eq. (41), c_{mn} is represented by the following expression.

$$\begin{aligned}c_{mn}&=\frac{1}{\pi}\int_0^{2\pi}\left\{\frac{2}{\pi}\int_0^{\pi}F(x, y)\cos 2mxdx\right\}\cos nydy\\&=\frac{1}{\pi^2}\left\{\int_0^{2\pi}\int_0^{\pi}F(x, y)\cos(2mx+ny)dxdy+\int_0^{2\pi}\int_0^{\pi}F(x, y)\cos(2mx-ny)dxdx\right\}\end{aligned} \tag{45}$$

And, d_{mn}, c'_{mn} and d'_{mn} are given by Eq. (46), (47) and (48) in similar operations to c_{mn}.

$$d_{mn}=\frac{1}{\pi^2}\left\{\int_0^{2\pi}\int_0^{\pi}F(x, y)\sin(2mx+ny)dxdy-\int_0^{2\pi}\int_0^{\pi}F(x, y)\sin(2mx-ny)dxdy\right\} \tag{46}$$

$$c'_{mn}=\frac{1}{\pi^2}\left\{\int_0^{2\pi}\int_0^{\pi}F(x, y)\sin(2mx+ny)dxdy+\int_0^{2\pi}\int_0^{\pi}F(x, y)\cos(2mx-ny)dydy\right\} \tag{47}$$

$$d'_{mn}=\frac{1}{\pi^2}\left\{\int_0^{2\pi}\int_0^{\pi}F(x, y)\cos(2mx+ny)dxdy-\int_0^{2\pi}\int_0^{\pi}F(x, y)\cos(2mx-ny)dxdy\right\} \tag{48}$$

From Eq. (36), Eq. (39) and Eq. (40), $F(x, y)$ is expressed as,

$$F(x,y)=\frac{1}{2}a_0(y)+\sum_{m=1}^{\infty}\left\{\frac{1}{2}c_{mo}\cos 2mx+\frac{1}{2}c'_{mo}\sin 2mx\right\}$$
$$+\sum_{m=1}^{\infty}\sum_{n=1}^{\infty}\left\{(c_{mn}\cos ny+d_{mn}\sin ny)\cos 2mx+(c'_{mn}\cos ny+d'_{mn}\sin ny)\sin 2mx\right\} \tag{49}$$

Inserting the relations of Eq. (45)$\sim$Eq. (48) into the coefficients in Eq. (49) and collecting like terms, $F(x, y)$ is rewritten as follows:

$$F(x,y)=\frac{1}{2}A_{00}+\sum_{n=1}^{\infty}(A_{on}\cos ny+B_{on}\sin ny)+\sum_{m=1}^{\infty}(A_{mo}\cos 2mx+B_{mo}\sin 2mx)$$
$$+\sum_{m=1}^{\infty}\sum_{n=\pm 1}^{\pm\infty}\{A_{mn}\cos(2mx+ny)+B_{mn}\sin(2mx+ny)\} \tag{50}$$

where,

$$A_{mn}=\frac{1}{\pi^2}\int_0^{2\pi}\int_0^{\pi}F(x,y)\cos(2mx+ny)\,dxdy \tag{51}$$

$$B_{mn}=\frac{1}{\pi^2}\int_0^{2\pi}\int_0^{\pi}F(x,y)\sin(2mx+ny)\,dxdy \tag{52}$$

$$(m=0,\ 1,\ 2,\ 3,\ \cdots\cdots,\quad n=0,\ 1,\ 2,\ 3,\ \cdots\cdots)$$

From Eq. (51) and Eq. (52), $A_{mn}+jB_{mn}$ is expressed as follows:

$$A_{mn}+jB_{mn}=\frac{1}{\pi^2}\int_0^{2\pi}\int_0^{\pi}F(x,y)\cdot\varepsilon^{j(2mx+ny)}dxdy \tag{53}$$

$$(m=0,\ 1,\ 2,\ 3,\ \cdots\cdots,\quad n=0,\ 1,\ 2,\ 3,\ \cdots\cdots)$$

References

1) H. S. Black: Modulation Theory, Ch. 17, D. Van Nostrand Co., New York, N. Y. (1953).
2) K. Miyakoshi, S. Hata and S. Minamoto: This bulletin, **A2,** 25 (1954).
3) S. Minamoto, K. Nohara and K. Miyakoshi: This bulletin, **A9, No. 1,** 31 (1960).